eIF4A RNA Helicase Associates with Cyclin-Dependent Protein Kinase A in Proliferating Cells and is Modulated by Phosphorylation

Bush, Maxwell S.; Pierrat, Olivier; Nibau, Candida; Mikitova, Veronika; Zheng, Tao; Corke, Fiona M. K.; Vlachonasios, Konstantinos; Mayberry, Laura K.; Browning, Karen S.; Doonan, John

Published in:
Plant Physiology

DOI:
10.1104/pp.16.00435

Publication date:
2016

Citation for published version (APA):
Bush, M. S., Pierrat, O., Nibau, C., Mikitova, V., Zheng, T., Corke, F. M. K., ... Doonan, J. (2016). eIF4A RNA Helicase Associates with Cyclin-Dependent Protein Kinase A in Proliferating Cells and is Modulated by Phosphorylation. Plant Physiology, 172(1), 128-140. https://doi.org/10.1104/pp.16.00435

eIF4A RNA Helicase Associates with Cyclin-Dependent Protein Kinase A in Proliferating Cells and Is Modulated by Phosphorylation[1][OPEN]

Maxwell S. Bush, Olivier Pierrat[2], Candida Nibau, Veronika Mikitova[3], Tao Zheng, Fiona M. K. Corke, Konstantinos Vlachonasios, Laura K. Mayberry, Karen S. Browning*, and John H. Doonan*

Department of Cell and Developmental Biology, John Innes Centre, Norwich NR4 7UH, United Kingdom (M.S.B., O.P., V.M.); Institute of Biological, Environmental, and Rural Sciences, Aberystwyth University, Gogerddan Campus, Aberystwyth SY23 3EE, United Kingdom (C.N., F.M.K.C., K.V., J.H.D.); Institute of Virology and Biotechnology, Zhejiang Academy of Agricultural Science, Hangzhou City, Zhejiang Province 310021, China (T.Z.); Aristotle University of Thessaloniki, Faculty of Science, School of Biology, Department of Botany, 54124 Thessaloniki, Greece (K.V.); and Department of Molecular Biosciences and Institute for Cell and Molecular Biology, University of Texas, Austin, Texas 78712 (L.K.M., K.S.B.)

ORCID IDs: 0000-0003-1755-1645 (K.V.); 0000-0001-6027-1919 (J.H.D.).

Eukaryotic initiation factor 4A (eIF4A) is a highly conserved RNA-stimulated ATPase and helicase involved in the initiation of messenger RNA translation. Previously, we found that eIF4A interacts with cyclin-dependent kinase A (CDKA), the plant ortholog of mammalian CDK1. Here, we show that this interaction occurs only in proliferating cells where the two proteins coassociate with 5′-cap-binding protein complexes, eIF4F or the plant-specific eIFiso4F. CDKA phosphorylates eIF4A on a conserved threonine residue (threonine-164) within the RNA-binding motif 1b TPGR. In vivo, a phospho-null (APGR) variant of the Arabidopsis (*Arabidopsis thaliana*) eIF4A1 protein retains the ability to functionally complement a mutant (*eif4a1*) plant line lacking eIF4A1, whereas a phosphomimetic (EPGR) variant fails to complement. The phospho-null variant (APGR) rescues the slow growth rate of roots and rosettes, together with the ovule-abortion and late-flowering phenotypes. In vitro, wild-type recombinant eIF4A1 and its phospho-null variant both support translation in cell-free wheat germ extracts dependent upon eIF4A, but the phosphomimetic variant does not support translation and also was deficient in ATP hydrolysis and helicase activity. These observations suggest a mechanism whereby CDK phosphorylation has the potential to down-regulate eIF4A activity and thereby affect translation.

The coordination of cell division (mitosis) with cell growth is a common attribute of most eukaryotic cells. While it is clear that key cell cycle regulators (such as the cyclin-dependent protein kinase A [CDKA]) are not necessary for cell growth per se (Dissmeyer et al., 2009; Gaamouche et al., 2010), the mechanisms coordinating growth and division remain largely obscure. Based on previous work where we found a physical association between eukaryotic initiation factor 4A (eIF4A) and CDKA (Hutchins et al., 2004), a protein required for cell size homeostasis and normal growth (Bush et al., 2015), we hypothesize that the coordination of growth and cell division may involve reversible phosphorylation of key components of the cellular machinery.

Cell and organ growth are profoundly dependent on protein production, a process that provides the building blocks for new cellular components. One of the first steps involves the binding of the cap-binding complex, eIF4F, to the 7-methylated GTP (m^7GTP) residue (cap) of the mRNA (Jackson et al., 2010; Valásek, 2012; Hinnebusch, 2014; Mead et al., 2014; Merrick, 2015). The eIF4F complex is composed of eIF4E (the cap-binding subunit) and eIF4G (an adaptor protein), to which a variety of accessory proteins bind, including eIF4A, eIF4B, and poly(A)-binding protein (PABP). Plants possess a unique form of the eIF4F complex, eIFiso4F, composed of eIFiso4G and eIFiso4E (Browning and Bailey-Serres, 2015). Numerous combinations of the plant cap-binding and adapter proteins are possible, but there are indications that the different combinations have different affinities for particular mRNAs (Carberry et al., 1991; Ruud et al., 1998; Gallie and Browning, 2001; Mayberry et al., 2009, 2011). mRNA discrimination between the various eIF4F complexes may be related to the interaction between the cap-binding subunit and the 5′-m^7G residue or how individual eIF4 components affect how the complex as a whole interacts with the mRNA (Mayberry et al., 2011).

eIF4A is the canonical DEAD box RNA-stimulated ATPase and helicase that facilitates translation initiation by unwinding long and complex 5′ untranslated region secondary structures common to many eukaryotic mRNAs (Rogers et al., 2002; Tuteja et al., 2008; Parsyan et al., 2011; Andreou and Klostermeier, 2013; Linder and Fuller-Pace, 2013; Marintchev, 2013; Lu et al., 2014; Fehler et al., 2014). eIF4A and the poorly conserved, enigmatic protein eIF4B bind to eIF4G or

eIFiso4G in plant cap-binding complexes (Browning and Bailey-Serres, 2015). The flexible, elongated shape of eIF4B presumably allows its simultaneous interaction with eIF3, eIF4G, eIFiso4G, eIF4A, PABP, and mRNA (Mayberry et al., 2009). eIF4B is phosphorylated during development, when protein translation rates are high (Le et al., 1998), and is a substrate for Casein Kinase2 (Dennis and Browning, 2009). Phosphorylation of eIF4B and PAPB is important for their interaction, which, in turn, enhances the ATPase and RNA helicase activity of eIF4A (Bi and Goss, 2000). Plant eIF4A is phosphorylated in response to heat stress and hypoxia (Webster et al., 1991; Le et al., 1998), and proteomic analysis of phosphorylation states under a variety of conditions suggests at least three phosphopeptides for eIF4A1 and four for eIF4A2 (Boex-Fontvieille et al., 2013; Umezawa et al., 2013; Wang et al., 2013; Wu et al., 2013; Zhang et al., 2013), as indicated by the PhosPhAt database (Heazlewood et al., 2008; Durek et al., 2010; Zulawski et al., 2013).

Arabidopsis (*Arabidopsis thaliana*) has at least 58 members of the DEAD box RNA helicase family (Boudet et al., 2001), of which three are *eIF4A* genes, named eIF4A1, eIF4A2, and eIF4A3. Whereas Arabidopsis eIF4A1 and eIF4A2 proteins are cytoplasmic and function in translation, the functionally distinct eIF4A3 protein is a dynamic member of the nuclear exon-junction complex (Koroleva et al., 2009). The amino acid sequence similarity of eIF4A1 and eIF4A2 is generally 90% to 95%, and there are nine highly conserved motifs, one of which, the RNA-binding motif 1b TPGR, also is a CDKA consensus phosphorylation site (Takeda et al., 2001).

eIF4A interacts physically with the cell cycle regulator CDKA, the Arabidopsis ortholog of CDK1 (Hutchins et al., 2004), and associates with four different cap complexes: eIF4F, CBP20/CBP80, and the plant-specific eIFiso4F and nCBP (Bush et al., 2009). Notably, eIF4A associated with the cap-binding complexes in proliferating cells only (Hutchins et al., 2004). In quiescent or differentiated cells, eIF4A is replaced by other RNA helicases. Mammalian eIF4 genes have received much attention recently as possible oncogenes (Montanaro and Pandolfi, 2004), and eIF4A has been identified as a target of the antiproliferative drugs pateamine (Bordeleau et al., 2006a) and hippuristanol (Bordeleau et al., 2006b) and is a promising target for the control of cancer (Stoneley and Willis, 2015). These observations suggest that eIF4A could play an evolutionarily conserved role in regulating protein translation during the cell cycle.

To test the hypotheses that eIF4A is regulated by phosphorylation, mediated by cell cycle related kinases, and that this phosphorylation may affect growth, we took several approaches to evaluate the effect of phosphorylation on eIF4A activity. We showed previously that the loss of *eIF4A1* gene function leads to reduced plant growth and dramatically decreased fertility (Bush et al., 2015). Here, we show that eIF4A associates with and is phosphorylated by CDKA in proliferating tissues and cells. In vitro kinase assays demonstrated that CDKA can phosphorylate wheat (*Triticum aestivum*) eIF4A1 at Thr-164, a residue involved in RNA binding and part of the CDKA phosphorylation (TPGR) consensus motif. Arabidopsis *eif4a1* mutants expressing a phosphomimetic version (EPGR) of the Arabidopsis eIF4A gene fail to complement the lack of eIF4A1, whereas the phospho-null version (APGR) complements as well as the wild-type version. The phosphomimetic mutation, T164E, abrogates eIF4A1 activities in vitro; consequently, this mutant protein was unable to support protein translation in a wheat germ translation assay depleted of eIF4A, supporting the idea that CDKA phosphorylation may negatively regulate translation during proliferation.

RESULTS

CDKA and eIF4A Interact during S, G2, and M Phases

The correlation between cell proliferation and eIF4A recruitment to the cap-binding complexes (Bush et al., 2009), together with the physical interaction of eIF4A and CDKA (Hutchins et al., 2004), prompted us to investigate the dynamics of this interaction in more detail. Quiescent cells (i.e. 8-d-old Arabidopsis cultures) were induced to reenter the cell cycle semisynchronously by Suc starvation followed by dilution in fresh medium containing Suc (Menges and Murray, 2002), and the cap-binding and associated proteins were isolated on m^{7}GTP-Sepharose over a defined time course. Some proteins, including eIFiso4E and CBP80, were present in the cap-binding complexes at all stages (Fig. 1A). However, the overall profile of cap proteins became

[1] This work was supported by the Biotechnology and Biological Sciences Research Council (grant no. BB/C507988/1 to J.H.D., M.B., and O.P. and ISIS program travel grant to O.P.), the FP7 Agronomics Program (grant no. 37704 to J.H.D., M.B., and T.Z.), the FP7 Capacities Program (grant no. 284443 to EPPN, which also supported K.V.), and the National Science Foundation (grant no. MCB1052530 to L.K. M. and K.S.B.).

[2] Present address: Cancer Therapeutics Department, Institute of Cancer Research, Sutton SM5 5NG, UK.

[3] Present address: Central European Institute of Technology, Kamenice 753/5, 625 00 Brno, Czech Republic.

* Address correspondence to kbrowning@cm.utexas.edu and john.doonan@aber.ac.uk.

The author responsible for distribution of materials integral to the findings presented in this article in accordance with the policy described in the Instructions for Authors (www.plantphysiol.org) is: John H. Doonan (john.doonan@aber.ac.uk).

M.S.B. and O.P. performed the cell cycle reentry and cell synchrony experiments and kinase assays; O.P. and L.K.M. performed the translation assays; M.S.B. performed the RNA helicase assays; V.M. performed the yeast two-hybrid experiments; eIF4A fusion proteins and peptides were cloned by O.P. and T.Z.; C.N., F.M.K.C., and K.V. mutated eIF4A genomic clones to phosphosite variants and produced and analyzed transformants; M.S.B. and J.H.D. wrote the article; K.S.B. edited the article; K.S.B. and J.H.D. obtained funding and supervised the project.

[OPEN] Articles can be viewed without a subscription.

www.plantphysiol.org/cgi/doi/10.1104/pp.16.00435

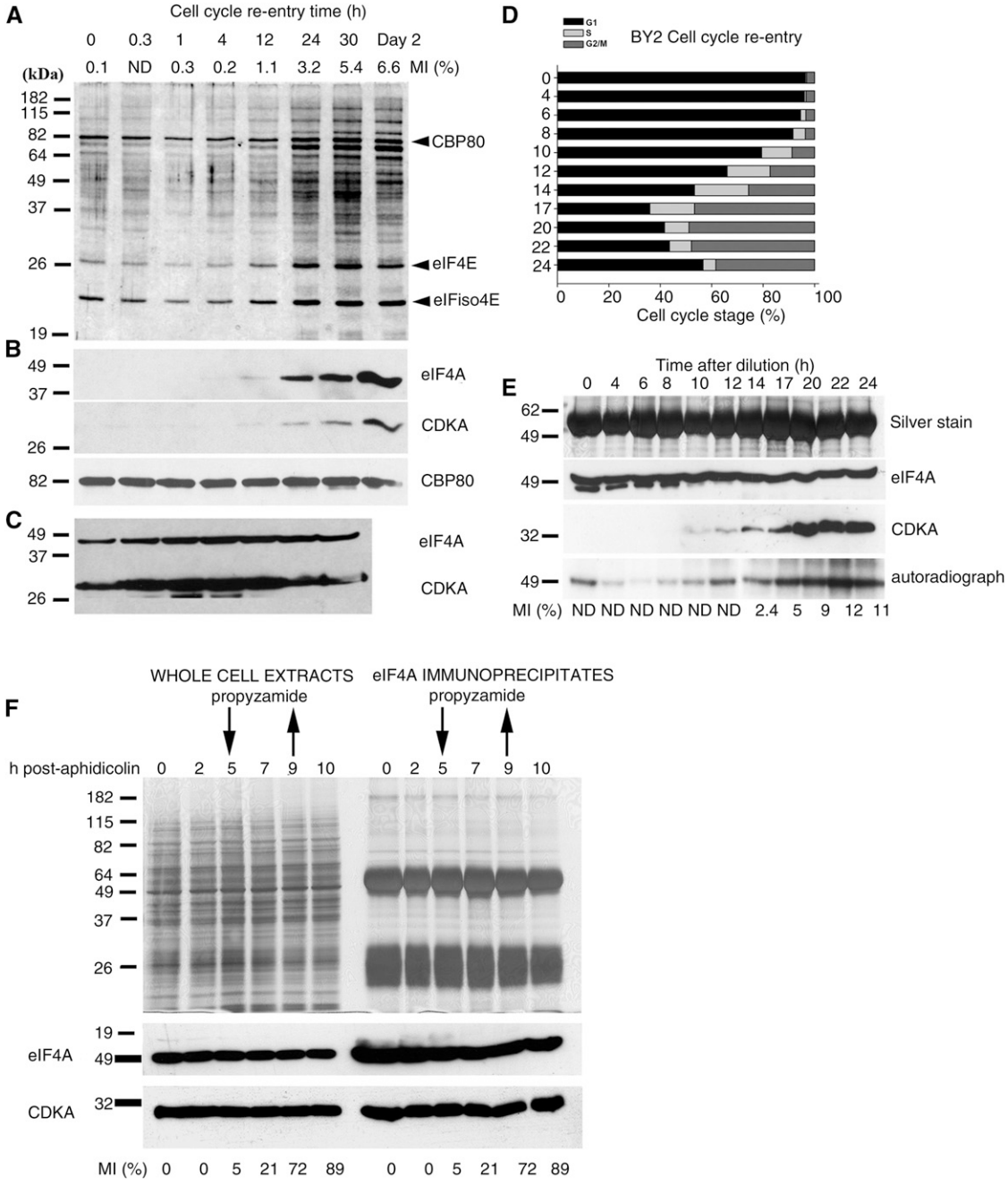

Figure 1. CDKA and eIF4A coassociation is maximal during M phase. A to C, Arabidopsis cultures were synchronized by Suc starvation/refeeding, and cap complexes were isolated at different times after refeeding. A, Silver staining of an SDS-PAGE gel showing the protein composition of cap complexes at different times (shown in hours at top). MI indicates the percentage of mitotic cells [mitotic index] at each time point. B, Western-blot analysis of samples shown in A using antibodies to eIF4A, CDKA, and CBP80; the latter was used to normalize protein loading at each time point. C, Western blots of soluble cell extracts. D to E, Ten-day-old BY2 cultures were semi-synchronized by dilution in fresh medium, and samples were taken at the times shown (hours after dilution). D, Flow cytometric analysis of nuclear DNA content. Cell cycle stage is shown in the key at top. E, Anti-eIF4A IP of samples shown in D. Gels are as follows: Silver stain, H-chain IgG polypeptide bands to show equal sample loading; eIF4A, western blot of eIF4A IPs probed with anti-eIF4A antibody (approximately equal amounts of eIF4A protein were immunoprecipitated); CDKA, western blot of eIF4A IPs probed with anti-CDKA showing that the level of coprecipitated CDKA increased gradually as the mitotic index increased (ND, not determined); autoradiograph, radiolabel incorporation after eIF4A IPs were subjected to a kinase assay in the absence of exogenous substrate. F, BY2 cells were treated with aphidicolin and propyzamide (arrows indicate the addition and removal of propyzamide) to achieve high synchronization (mitotic index up to 89%); whole-cell extracts (left) and eIF4A immunoprecipitates (right) were then prepared for SDS-PAGE and anti-eIF4A IPs. At top are silver-stained gels. Western blots (bottom) were probed with anti-CDKA and anti-eIF4A antibodies.

more complex with increasing time after the readdition of Suc, particularly from about 12 h, when the mitotic index started to increase. By 24 h after release, the profile of proteins was similar to that isolated from 2-d-old proliferating cells. eIF4A and CDKA first became detectable by western blotting in cap complexes after 12 h (Fig. 1B). Temporal corecruitment of the two proteins into cap complexes was independent of the amount of soluble eIF4A and CDKA present in the protein extracts (Fig. 1C).

To determine if the CDKA-eIF4A interaction occurs at a particular stage of the cell cycle, synchronized BY2 tobacco (*Nicotiana tabacum*) cell cultures were used because they give higher levels of synchrony compared with Arabidopsis cultures. After subculturing into fresh growth medium, the cultures were sampled every 2 to 3 h for 24 h and examined by flow cytometry to determine cell cycle stage (Fig. 1D) or processed by eIF4A immunoprecipitation (IP) and western blotting (Fig. 1E). Under these conditions, cells begin to enter S phase at 8 to 10 h, as judged by flow cytometric measurement of nuclear DNA content, and begin to enter M phase at 14 to 17 h, as judged by 4′,6-diamino-phenylindole staining. CDKA was initially detected coprecipitating with eIF4A 10 h after subculture (Fig. 1E), when approximately 20% of the BY2 cells were in either S or G2 phase (Fig. 1D). The amount of CDKA detected in the eIF4A IPs gradually increased, leveling off at 20 h and subsequent times, when up to 60% of cells were in S or G2 phase and the mitotic index was greatest. This suggested that the interaction begins during S or G2 phase and may reach a peak during G2 or M phase, during which time CDKA activity increases. The level of eIF4A phosphorylation correlates with the amount of coprecipitating CDKA (Fig. 1E, autoradiograph), except at very early time points. During the early time points (0–10 h), a minor eIF4A band gradually merges with the major band just as the CDKA interaction becomes detectable (10 h in Fig. 1E). This, together with the labeling of eIF4A at the early time point, very likely represents differential phosphorylation events of eIF4A at different sites by an unidentified kinase.

To test whether the association of eIF4A and CDKA was specific to G2/M, we synchronized BY2 cells with sequential aphidicolin and propyzamide treatments (Fig. 1F). Aphidicolin is a specific inhibitor of DNA polymerase and blocks the cell cycle at early S phase. Propyzamide is an herbicide that disrupts microtubules and, when applied after aphidicolin treatment, prevents cells released from the S phase block from completing mitosis; this double block in the cell cycle leads to high levels of cell synchrony. This experiment shows that the CDKA-eIF4A interaction occurs in cells from all time points after release from the aphidicolin block (0 h) and, therefore, is not dependent on mitosis per se. The potential for CDKA and eIF4A proteins to interact physically was further supported by yeast two-hybrid assays (Supplemental Fig. S1). Based on the ability of the yeast cells to grow on selective medium, pairwise tests of CDKA with various components of the eIF4 complex indicated that CDKA was able to interact with both eIF4A1 and eIF4A2. To evaluate the specificity of the interaction, we undertook pairwise tests using eIF4A and three other CDKs, CDKB, CDKC, and CDKD. Positive interaction was obtained with CDKB2.1, a plant-specific mitotic kinase, but not with CDKC or CDKD. Interestingly, interactions between CDKA and CDKB2.1 with eIF4E also were observed in the two-hybrid assay. Other subunits, eIF4B, eIFiso4E, eIFiso4G, or eIF4G (Supplemental Fig. S1), did not interact. However, we did not find any evidence for the phosphorylation of eIF4E or other eIFs in our CDKA kinase assays. It should be noted that there is a conserved site within CDKA (YRAPEILL), which is similar to the canonical 4E binding site (YxxxxLφ) found in eIF4G and other eIF4E-binding proteins (Sonenberg and Gingras, 1998) and may be the cause of the interaction in the two-hybrid assay. The function of this interaction is not known but could represent an uncharacterized regulatory interaction that is specific for eIF4E, since eIFiso4E did not interact, or the interaction may be a false positive from the yeast two-hybrid assay.

eIF4A Is Phosphorylated at Thr-164 by Mitotic Human and Plant CDKs in Vitro

We previously found that eIF4A coprecipitated with a roscovitine-sensitive histone H1 kinase activity similar to that observed for purified CDK-cyclin B complexes (Hutchins et al., 2004). To determine if eIF4A is a substrate of CDKA, we used eIF4A IPs (from extracts made with proliferating Arabidopsis cells) in kinase assays containing different concentrations of roscovitine, a specific CDK inhibitor (Fig. 2A). A single protein band, with a migration profile consistent with it being eIF4A, was strongly phosphorylated (arrowhead in Fig. 2A). Kinase activity in the IPs was eliminated by 0.5 and 5 μM roscovitine, indicating the presence of an active CDK. To test whether eIF4A phosphorylation was restricted to actively dividing cells, we used IPs from 4- and 6-d-old Arabidopsis cells in kinase assays, separated by SDS-PAGE, transferred the proteins to nitrocellulose to expose them to film, and then probed the membrane with the anti-eIF4A antibody (Fig. 2B). Immunodetectable eIF4A colocalized exactly with the radioactive band in the day-4 IP (proliferating cells) but not in the day-6 IP, despite using an increased loading of eIF4A protein. This observation is consistent with our previous finding that eIF4A and CDKA do not interact after culture day 5 (Hutchins et al., 2004).

A single consensus CDK phosphorylation motif is predicted in eIF4A1 and eIF4A2 from the consensus phosphorylation site, S/TPXK/R (Takeda et al., 2001), and this sequence is conserved in eIF4A sequences across species (Supplemental Fig. S2). The PhosPhAt database does not show any peptides that correspond to the CDKA site, suggesting that, under the conditions in the proteomic studies, the peptide was not identified

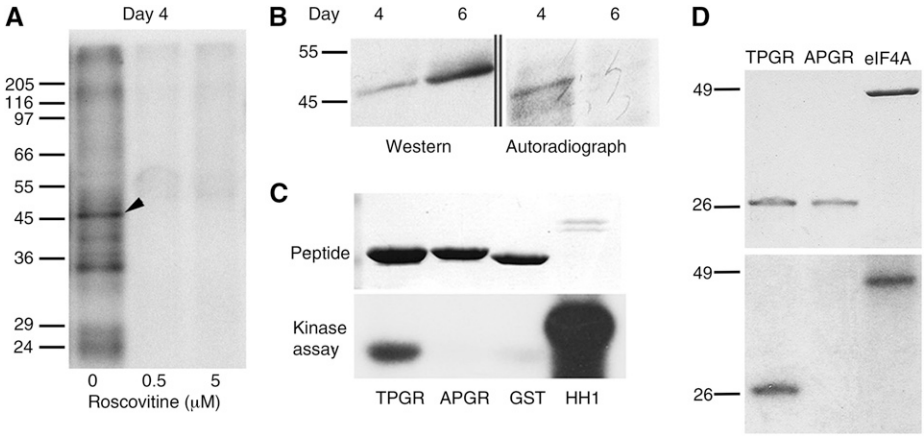

Figure 2. eIF4A is a substrate for a roscovitine-sensitive kinase. A, Autoradiograph of anti-eIF4A IPs from 4-d-old Arabidopsis cells. The IPs were subjected to a kinase assay ± the CDKA inhibitor roscovitine in the absence of exogenous substrate. The arrowhead indicates a phosphorylated protein with an M_r identical to that of eIF4A. B, Anti-eIF4A IPs used in kinase assays were separated by SDS-PAGE, transferred to nitrocellulose, probed with an anti-eIF4A antibody (Western), and exposed to film (Autoradiograph). C, Kinase assay using human CDK1-cyclin B to phosphorylate GST-tagged eIF4A peptides containing the conserved wild-type CDK phosphorylation site (TPGR) and a mutated phospho-null APGR version. The phospho-null form is not phosphorylated. Histone H1 was used as a control. D, Kinase assays using CDKA immunoprecipitated from 2-d-old Arabidopsis cell suspension cultures to phosphorylate GST-tagged peptides (TPGR and APGR) and recombinant wheat eIF4A protein (eIF4A). Top, Coomassie Blue-stained gel; bottom, autoradiograph.

for technical reasons or the CDKA modification is rare and/or highly transient in the tissues analyzed. However, inspection of the mammalian phosphoproteome databases http://hprd.org and http://www.phosphosite.org indicates that the same residue is phosphorylated and is in a good consensus site for CDK phosphorylation, suggesting a conserved function for this phosphorylation. Possible reasons for the absence of this modification in the plant databases include the generally low coverage of the plant phosphoproteome compared with the mammalian, where many more studies are available, the low abundance of proliferating and mitotic cells in most plant tissues used so far for systematic phosphoproteomics, or that the proportion of eIF4A phosphorylated on this site is relatively low. In our hands, only radiolabel methods routinely detected phosphorylation, suggesting that the level of phosphorylation by CDKA is low. To investigate if the Thr at this site can be phosphorylated by CDKA, we used commercial recombinant human CDK1-cyclin B (a mitotic CDK homologous to CDKA) to phosphorylate glutathione *S*-transferase (GST)-tagged (29-mer) oligopeptides containing the TPGR sequence of eIF4A or a phospho-null version, APGR (Fig. 2C). The peptide containing the wild-type TPGR motif is phosphorylated, whereas the APGR-containing peptide and GST tag alone are not (Fig. 2C). In addition, CDKA, immunoprecipitated from 2-d-old Arabidopsis cell suspension cultures, was able to phosphorylate both the TPGR peptide and a recombinant eIF4A protein, but the phospho-null APGR peptide was not phosphorylated (Fig. 2D). These data indicate that eIF4A Thr-164 can be phosphorylated by mitotic human and plant CDKs.

A Phosphomimetic Mutation at eIF4A Thr-164 Lacks eIF4A1 Activity in Vivo

Native AteIF4A, as isolated by IP, was inactive as a helicase in our in vitro assay, so we were unable to test the effect of phosphorylation by CDKA in vitro. Therefore, we tested whether the phospho-null (APGR) and phosphomimetic (EPGR) versions of AteIF4A1 could complement an *eif4a1* homozygous mutant (Bush et al., 2015). Transgenic lines were genotyped by diagnostic PCR for the wild-type and transfer DNA (T-DNA) alleles of the endogenous *eIF4A* genes, and the transgenic phosphosite-variant versions were reisolated by PCR and sequenced to confirm their identities. Of the 18 T1 *eif4a1/eif4a1* lines identified carrying the wild-type (TPGR) version, 16 were complemented, as judged by reversal of the late flowering time and short silique length, while two remained semi-sterile and late flowering. Similarly, with the phospho-null (APGR) version, 17 out of 18 lines were fully complemented. However, for 15 lines carrying the phosphomimetic (EPGR) version, none were complemented, and all displayed the slow-growing, late-flowering, and decreased-fertility *eif4a1* phenotype.

To evaluate the functionality of the different eIF4A variants, we quantified various aspects of the plant phenotype that we reported previously to be affected (Bush et al., 2015) as well as flowering time. Typical phenotypes for transgenic lines are shown in Figure 3, A and B (vegetative), and Figure 3C (floral transition). Impaired rosette growth (Bush et al., 2015) is fully repaired by transformation of the wild-type (TPGR) version and substantially repaired by the phospho-null (APGR) version of the Arabidopsis *eIF4a* gene, as shown by dynamic measurement of plant growth (Fig. 3B).

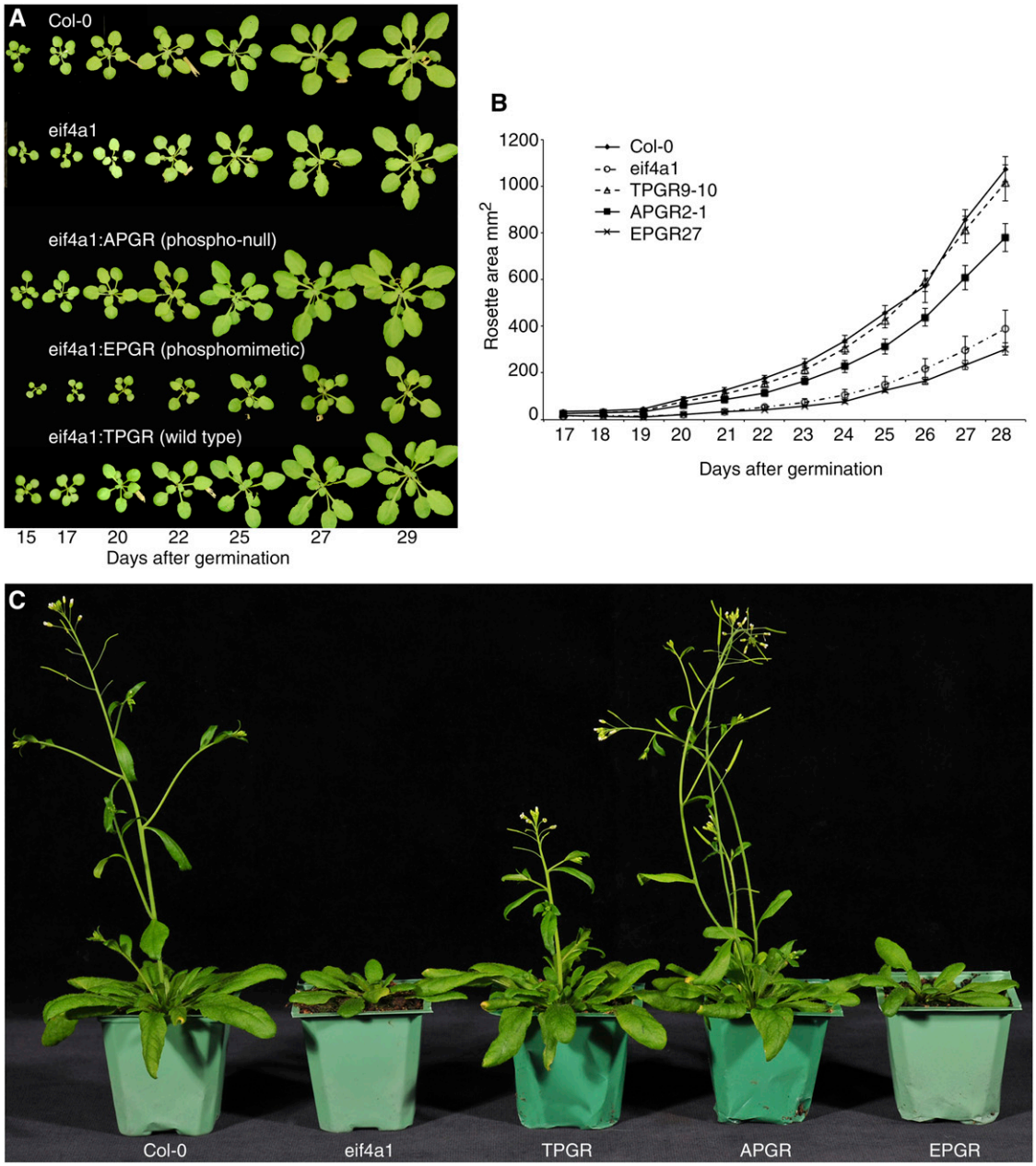

Figure 3. Functional complementation of the *eif4a1* mutant with eIF4A1 phosphovariants. A, Randomly selected examples of rosettes from *eif4a1* mutants complemented with the three eIF4A1 phosphovariant transgenes and Col-0 wild-type plants. B, Average rosette areas of Col-0 and *eif4a1* mutants complemented with the three transgenes grown over a developmental period of 12 d. *eif4a1* mutants transformed with the EPGR phosphomimetic transgene are not rescued from the mutant growth condition, unlike those mutants transformed with the APGR or TPGR genes. $n = 8$ for each genotype at each time point; error bars represent SE. C, Homozygous *eif4a1* mutants transformed with full-length genomic *AteIF4A1* genes were grown simultaneously in the greenhouse under long-day conditions. Mutant plants transformed with a phosphomimetic construct (EPGR) resemble the mutant phenotype (*eif4a1*), whereas transformants expressing the wild-type eIF4A gene (TPGR) or the phospho-null version (APGR) both complement.

The phosphomimetic (EPGR) version does not complement, and indeed, some phosphomimetic transgenic lines develop slightly more slowly than the original *eif4a* mutant, although this is not significant. The wild-type (TPGR) and phospho-null (APGR) versions of the Arabidopsis *eIF4a* gene can complement the slow apical meristem growth, as measured by the number of leaves at different ages (Fig. 4, A–C), reduced fertility (Fig. 4, D–F), and reduced root size (Supplemental Fig. S3A), whereas the phosphomimetic

(EPGR) version did not complement any of these phenotypes. The difference in root size can be accounted for in part by slower germination (delay of about 1 d in the mutant and transgenic phosphomimetic lines) and in part by slower growth rate (Supplemental Fig. S3B).

Floral Initiation Is Delayed by the Loss of eIF4A1

Notably, the *eif4a1* mutant has a pronounced late-flowering phenotype (Fig. 3C; Supplemental Fig. S4A) that was not observed in an analogous mutant in *Brachypodium* spp. (Vain et al., 2011). However, eIF4A has been implicated as a candidate gene for a flowering time quantitative trait locus in maize (*Zea mays*; Durand et al., 2012). We hypothesized that the flowering time phenotype may involve eIF4A-dependent expression of FLOWERING LOCUS C (FLC), a MADS box transcription factor that inhibits the floral transition, and/or other genes in this pathway. We assessed the expression of the negative regulator *FLC* and of the positive

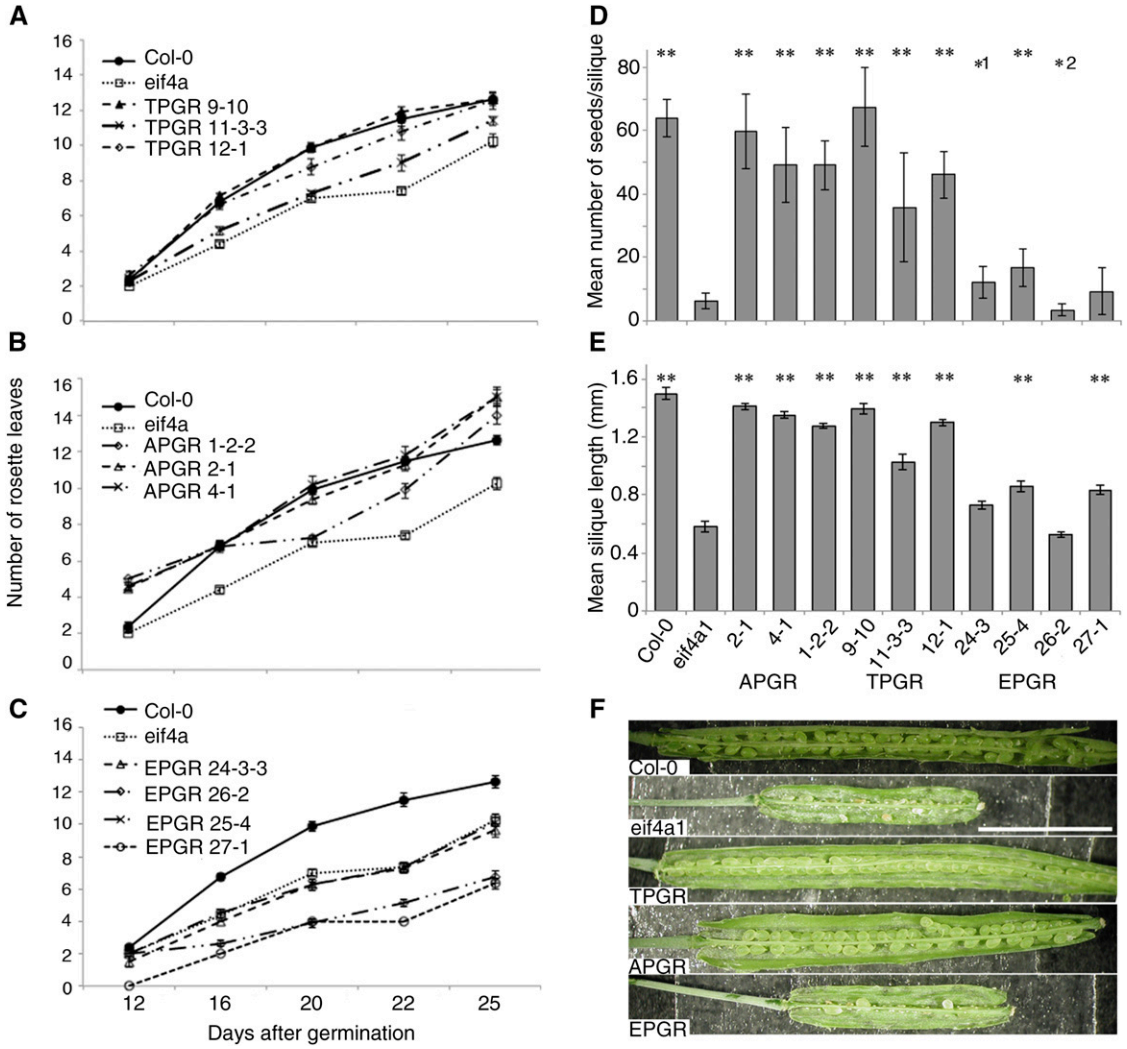

Figure 4. Phenotypic analysis of transformed *eif4a1* mutant plants. A to C, Vegetative growth measured as the mean number of rosette leaves produced after 25 d of growth in long days. A, *eif4a1* homozygous mutant plants expressing a full-length genomic wild-type eIF4A1 gene (TPGR) rescue the mutant phenotype (*eif4a1*) to wild-type levels (Col-0). B, Mutants expressing the phospho-null eIF4A1 gene (APGR) also recover the wild-type growth rate. C, The phosphomimetic (EPGR) transformants grow leaves at a rate similar to or slower than the *eif4a1* mutant plants. D, The strong ovule-abortion phenotype of the *eif4a1* homozygous mutant (*eif4a1*) is rescued by transformation with the wild-type version (TPGR) or the phospho-null version (APGR) of the full-length genomic eIF4A1 gene but not by the EPGR phosphomimetic variant. E, The short siliques typical of the *eif4a1* mutant recover the normal wild-type length (Col-0) only after transformation with the TPGR or APGR phosphovariants but not the phosphomimetic EPGR variant. Two-tailed, unpaired Student's *t* tests were calculated with Genstat 16: double asterisks indicate significant differences ($P < 0.001$) from the *eif4a1* mutant, and *1 and *2 indicate $P < 0.005$ and $P < 0.01$, respectively. F, Images of *eif4a1* mutant siliques rescued to Col-0 status by transformation with the wild-type or T164A AteIF4A1 genes.

regulators *FLOWERING LOCUS T* (*FT*) and *SUPRESSOR OF CONSTANS1* (*SOC1*; Zacharaki et al., 2012) using reverse transcription (RT)-PCR. We observed that FLC transcripts are more abundant in the *eif4a1* mutant compared with Columbia-0 (Col-0), the positive regulator SOC1 is less abundant than in Col-0 grown under equivalent daylengths, while the positive regulator FT could not be detected in the mutant under long days (Supplemental Fig. S4B), in keeping with the observed flowering time phenotypes. While this does not reveal the primary target of eIF4A in flowering time control, the FLC pathway is regulated at several levels, including RNA processing (Quesada et al., 2003). However, the effect could be indirect, through cell proliferation and growth, as these processes are retarded in *eif4a1* mutants and are essential to produce the inflorescence and floral meristems.

Both the wild-type and the phospho-null versions of the eIF4A1 gene complement the flowering time defect, but the phosphomimetic version does not (Fig. 3C). Quantitative analysis of flowering time, as measured by days to flowering, supports this, and although there is variation between individual transgenic lines, all the transformants carrying wild-type or phospho-null eIF4A constructs flowered significantly earlier than the mutant or phosphomimetic lines (Supplemental Fig. S4C). The differential complementation could be due to low expression of the phosphosite variants compared with the wild-type gene. RT-PCR of the different lines indicated that all transgenes were expressed at variable levels compared with the wild-type gene, although the lowest expression was by the TPGR line, which complemented the *eif4a1* phenotype, suggesting that expression is not the issue (Supplemental Fig. S5).

The eIF4A Phosphomimetic (EPGR) Protein Is an Inactive RNA Helicase

In vivo assessment of phosphosite variants in Arabidopsis was technically impossible due to interference by eIF4A2, produced by a highly homologous paralog. Therefore, further in vitro biochemical analysis using recombinant proteins was carried out to assess directly the activity of the phosphosite variants. Wheat eIF4A (Mayberry et al., 2007) was used, since recombinant Arabidopsis eIF4A1 formed inclusion bodies. The CDKA phosphorylation site is perfectly conserved in wheat eIF4A, and the phosphosite mutant versions of wheat eIF4A were constructed, as was a version containing a mutation, E191Q, in the DEAD box motif that was reported previously to be functionally inactive in mammalian eIF4A (Pause and Sonenberg, 1992). All forms of the purified proteins were subjected to circular dichroism analysis and showed similar levels of protein folding. To evaluate whether the mutations could affect helicase activity, we quantitatively compared the ATP hydrolysis and helicase activities of mutant versions with wild-type wheat protein eIF4A in vitro (Fig. 5, A–C). In vitro, eIF4A protein is an active ATPase in the presence of poly(A) RNA (Fig. 5A). The phospho-null (APGR) form showed wild-type-like activity even in the absence of poly(A) RNA, while the phosphomimetic version (EPGR) was inactive to a similar extent as the DEAD box mutation E191Q mutant (Fig. 5B). In vitro helicase activity as detected by the presence of RNA monomers confirmed that the wild-type and APGR forms are active helicases, while no activity was detected for the EPGR phosphomimetic form, which was similar to the result obtained with wild-type wheat eIF4A that had been inactivated by boiling (Fig. 5C).

The eIF4A Phosphomimetic (EPGR) Protein Does Not Support in Vitro Translation

We then tested the ability of these three different wheat eIF4A protein versions to quantitatively restore translational capacity to an eIF4A-depleted wheat germ in vitro translation extract, prepared according to a method described previously for the depletion of eIF2 (Benkowski et al., 1995). First, we verified that our eIF4A-depleted translation assay was dependent on added wild-type wheat eIF4A. eIF4F (composed of the subunits eIF4E and eIF4G) and eIF4B were supplemented, as these factors were codepleted along with eIF4A, particularly eIF4F, which is the least abundant in wheat germ lysate (eIF4A is present in a greater than 30-fold molar excess relative to eIF4G; Browning et al., 1990). We found that both the wild-type and phospho-null proteins were able to support the translation of transcripts in a dose-dependent manner, with the wild type being the more active of the two based on the addition of equivalent amounts of protein (Fig. 5D). In contrast, the phosphomimetic version was completely unable to support in vitro translation, similar to the DEAD box mutant E191Q.

Previously it had been shown that protein translation is quantitatively dependent on the amount of eIF4A added back and that different eIF4F complexes may be discriminatory for certain mRNA species (Mayberry et al., 2011). To test the idea that high eIF4A levels might be required for the efficient translation of cell cycle-related transcripts, we compared the ability of the wheat germ system and different eIF4A variants to translate three different plant mRNAs: a representative storage protein, barley α-amylase (BAA), a heat shock 21 protein (AtHSP21), and a cell cycle regulator (AtCyclin D3.1). Consistent with the idea that cell cycle-related transcripts might be more sensitive to eIF4A level/activity, the AtCyclin D3 mRNA required approximately 3.5 μg of eIF4A to reach half-maximal translation compared with BAA mRNA, which required approximately 1.5 μg, and the HSP21 mRNA, which required the least at less than 0.5 μg (Fig. 5D). The amount of phospho-null eIF4A required for half-maximal translation of BAA mRNA increased approximately 2-fold to approximately 3 μg and had an approximately 3-fold lower maximal translation. Interestingly, the maximal translation reached by the

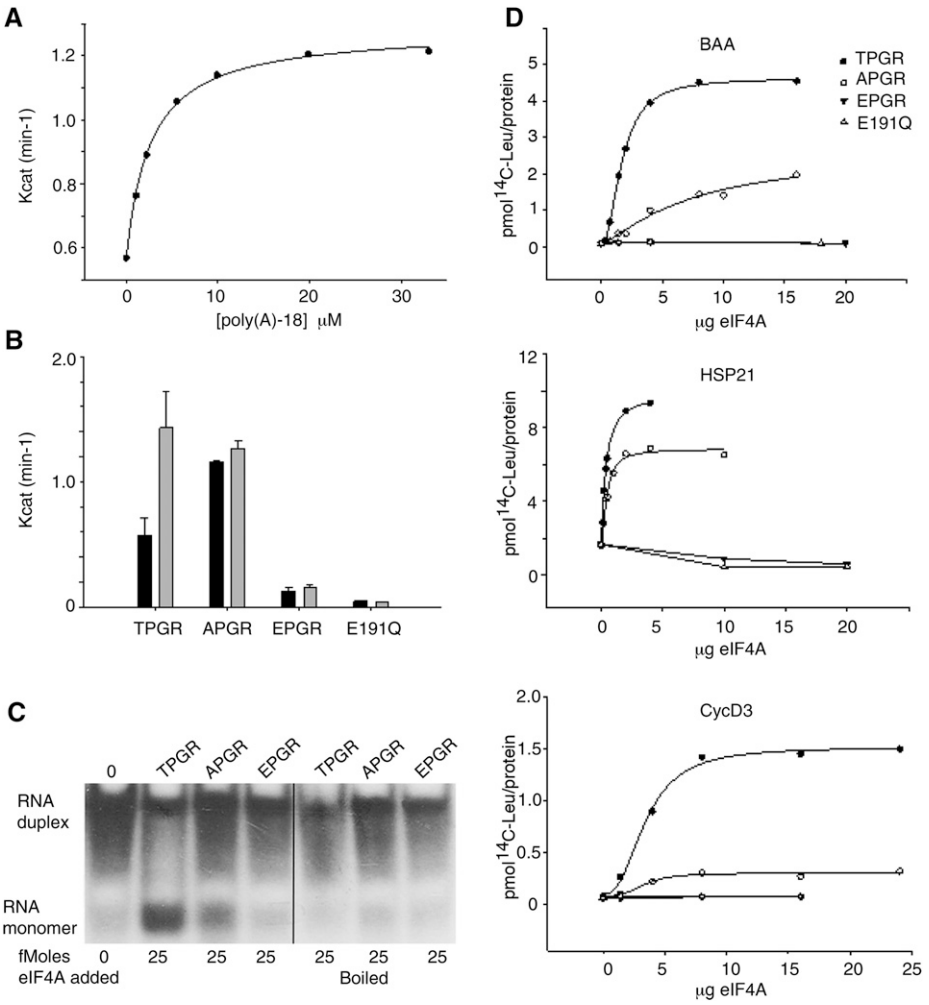

Figure 5. A phosphomimetic mutation (EPGR) but not a phospho-null mutation (APGR) abrogates the activities of recombinant wheat eIF4A1 protein. A, Stimulation of wild-type ATPase activity by poly(A) 18-mer RNA at pH 6. B, ATPase activity of wild-type and mutant wheat enzymes with (black columns) or without (gray columns) 7 μM poly(A) RNA. Phosphomimetic EPGR is nearly as inactive as E191Q (DEAD→DQAD), whereas phospho-null APGR showed wild-type-like activity, regardless of the presence or the absence of RNA. C, In vitro RNA helicase assay. RNA duplexes were assayed with no added eIF4A (0), wild-type wheat eIF4A (TPGR), or two mutated wheat forms, APGR (phospho-null) or EPGR (phosphomimetic). eIF4A helicase activity is evident by the appearance of the RNA monomer. The three assays at right, which show no activity, used wheat eIF4A that had been inactivated by heating in boiling water. D, Depleted wheat germ extract was supplemented with recombinant wild-type or mutant wheat eIF4A and tested for translation of different capped mRNAs: BAA, AtHSP21, and AtCyclin D3;1. Incorporated radioactivity in pmol was normalized per amount of Leu present in each protein. Each experiment was carried out in triplicate, and two experiments were averaged; SD values between two independent experiments (10%–25%) are not represented for clarity.

AtCyclin D3 mRNA in the presence of the phospho-null eIF4A was reduced by approximately 5-fold, but the amount of eIF4A required for half-maximal translation remained the same as in the wild type (approximately 3.5 μg). HSP21 mRNA was the least affected by the phospho-null eIF4A, with only an approximately 1.4-fold reduction in maximal translation and little change in the amount required to reach half-maximal translation. It would require testing of other cell cycle mRNAs to determine if there is a special sensitivity to the phospho-null state of eIF4A, but it is an intriguing possibility for regulating a large number of mRNAs involved in a specific process.

These results indicate that the phospho-null version of the eIF4A protein retains both helicase and translation activity, although these activities may be partly reduced. However, introduction of the phosphomimetic mutation abolishes activity in an in vitro translation assay, corroborating our in planta observations that the phospho-null version of eIF4A protein can rescue the eIF4A mutant phenotype whereas the phosphomimetic version cannot. Furthermore, these results suggest that phosphorylation of the CDKA consensus phosphorylation site impacts the ability of eIF4A to participate in the initiation of translation.

DISCUSSION

The molecular basis of the relationship between cell growth and cell proliferation in plant cells remains obscure. Down-regulation of CDKA activity in tobacco (Hemerly et al., 1995) and Arabidopsis (Gaamouche et al., 2010) leads to uncoupling of the two processes, whereby loss of CDKA strongly inhibits cell proliferation, but cell growth is not particularly perturbed and the resultant cells are actually larger. Taken together, these observations indicate that CDKA is not required for cell growth per se and, therefore, may not be required for protein translation. Indeed, evidence from animals indicates that CDK1 actively and specifically inhibits protein translation during mitosis (Pyronnet et al., 2001) through the phosphorylation and activation of 4E binding proteins (4EBP) that modulate cap-dependent translation through sequestration of eIF4G from binding to eIF4E. Mammalian eIF4A is subject to regulation by CDK1 at mitosis by the phosphorylation

of an interacting protein, eIF4G1, which alters eIF4A binding to mRNA (Dobrikov et al., 2014). Currently, there is no evidence for either of these mechanisms in plants: no ortholog of 4EBP has been recognized (Pierrat et al., 2007; Browning and Bailey-Serres, 2015), and our results suggest that eIFG is probably not a binding partner of CDKA. Therefore, the regulation of translation during the plant cell cycle remains an open question.

Our results suggest that the eIF4A-CDKA interaction could provide an alternative molecular pathway for controlling translation in proliferating tissues, thereby contributing to cell size homeostasis in meristems. Root growth is slower in the knockout *eif4a1* mutant, probably due to the reduced number of cell divisions (Bush et al., 2015). Leaf initiation also is slightly delayed but leaves grow to nearly normal size, consistent with the observation that the eIF4A association with the 5′ cap complex is strongly correlated with proliferation in both cell cultures and tissues but that eIF4A is no longer detectable in the cap complex of postproliferative cells growing by cell expansion (Bush et al., 2009).

The question then arises how the interaction might alter the function of the partner proteins. The most likely scenario is that eIF4A is a CDKA substrate, since it contains one highly conserved eIF4A TPGR motif that is known to be phosphorylated in vivo in mammalian cells. Although we do not exclude the possibility that other sites also could be phosphorylated by CDKA or other kinases, we show that the Thr residue within this motif is subject to CDKA phosphorylation and that these residues are important for function both in vivo and in vitro. Plant phosphoproteome databases currently do not report a similar modification, and we were only able to detect the modification using radioactive incorporation of phosphate, suggesting either that only a small proportion of the eIF4A is modified or that the modification is transient. However, the functional significance of the modification is supported by the observation that a phosphomimetic substitution at this site lacks ATP hydrolysis and helicase activity, does not support translation in vitro, and also fails to complement the *eif4a1* mutant. The introduction of a negatively charged residue in the phosphomimetic mutant, therefore, reduces eIF4A activity, indicating that phosphorylation of this site has the potential to downregulate activity. Crystal structures of *Saccharomyces cerevisiae* eIF4A (Benz et al., 1999) suggest that motif 1a (PTRELA, GG, and TPGR) and the closely positioned SAT domain bind RNA through a cluster of positive charges on the surface of this region of the protein. The phosphorylation of the Thr residue in TPGR, or changing TPGR to EPGR, would introduce a negative charge, and this would possibly disrupt the cluster of positive charges. We speculate that this may bring about a conformational change or alter the interaction with RNA, either of which could affect eIF4A function. This would have a very similar effect to that reported by Dobrikov et al. (2014), where eIF4A RNA binding is subject to mitotic regulation by CDK1, albeit indirectly via the phosphorylation of eIF4G1. Conversely, an uncharged residue that cannot be phosphorylated (phospho-null) retains activity in vitro and is able both to complement the insertion mutant in Arabidopsis and support translation in eIF4A-depleted wheat germ extracts, albeit at reduced rates. This indicates that the protein can tolerate amino acid substitutions at this site, that phosphorylation is not required for activity, and supports the idea that phosphorylation could negatively impact activity. Therefore, phosphorylation would provide a mechanism to negatively regulate translation, with a different target but analogous to the CDK1-eIF4G mechanism reported for mammalian cells (Dobrikov et al., 2014).

The PhosPhAt database indicates that eIF4A is phosphorylated on at least two other sites (Heazlewood et al., 2008; Durek et al., 2010; Zulawski et al., 2013) by unknown kinases, and a further comprehensive study is required to compare the activities of eIF4A1 phosphorylated at combinations of these different sites. There is evidence from our study that other kinases in plant cell extracts can phosphorylate eIF4A, as eIF4A is phosphorylated in IPs from Suc-starved cells (Fig. 1E). CDKA protein is not detectable in IPs from these time points, and it is possible that phosphorylation at other site(s) in eIF4A by as yet unknown kinases could modulate CDKA interaction with eIF4A.

Both eIF4A and CDKA are relatively abundant proteins, yet our previous data (Hutchins et al., 2004) suggest that only a small proportion of each interact. From estimations based on western blotting and of the proportion of CDKA kinase activity associated with eIF4A, the amount of CDKA involved is similar to that bound to cyclin D, itself a low-abundance CDKA-interacting protein. As phosphoproteomics becomes more sensitive and quantitative, it should be possible to measure the ratio of phosphorylated to unphosphorylated eIF4A and follow changes during the cell cycle and in response to external stresses.

eIF4A is considered to be a general translation factor that could affect the expression of many genes. Although there are many structurally similar helicases, eIF4A was the only helicase that could be detected as associated with the cap complex of proliferating Arabidopsis cells. In nonproliferating cells that are still capable of growth through cell expansion, eIF4A remains an abundant cellular protein but no longer associates with the cap complex and is replaced by other RNA helicases (Bush et al., 2009). This indicates that the composition of the cap complex is dynamic and suggests that eIF4A may be critical for translation during cell proliferation. Consistent with this idea, we find that selected aspects of growth and development are differentially sensitive to the level and phosphorylation status of eIF4A. One possibility is that the interaction of eIF4A and CDKA could be limited by the availability of adapter/scaffold proteins, such as cyclin proteins (Ubersax and Ferrell, 2007; Kõivomägi et al., 2011). An alternative, but not necessarily exclusive, mechanism is a temporal-spatial restriction that has been reported previously for other CDK interactions (Obaya and Sedivy, 2002), and translation is known to be

spatially heterogenous (Jung et al., 2014). Mitotic proteins, for example, are locally translated in at least some cell types (Eliscovich et al., 2008).

Translation in plants is likely modulated by reversible protein phosphorylation involving a number of kinases acting on diverse components, although the exact nature of the kinases and phosphorylation events is largely uncharacterized (Roy and von Arnim, 2013). Our results support the hypothesis that the phosphorylation of eIF4A by cell cycle-related kinases, such as CDKA and CDKB, plays a role in growth control and development.

MATERIALS AND METHODS

Affinity Matrix Isolation and Kinase Assays

Arabidopsis (*Arabidopsis thaliana*) anti-eIF4A IP, isolation of cap complexes, silver staining, SDS-PAGE, and western-enhanced chemiluminescence immunodetection were performed according to Bush et al. (2009). CDKA was detected using a monoclonal mouse antibody to the PSTAIRE motif (Sigma). For kinase assays, the procedure of Hutchins et al. (2004) was used. Kinases were preincubated with the CDK inhibitor roscovitine before addition of the substrate. Each 20-μL kinase reaction was incubated for 30 to 60 min at 30°C in kinase buffer containing 0.1 mM ATP and 74 kBq [γ-^{32}P]ATP. GST-tagged eIF4A peptides (VREDQRILQAGVHVVVGTPGRVFDMLKRQ) with the indicated version of eIF4A and peptides with wild-type (TPGR), phospho-null (APGR), or phosphomimetic (EPGR) phosphorylation sites were made by conventional cloning using primers eIF4Apeptide F and eIF4Apeptide R and cloned into pGEX4T for expression of GST-tagged peptides in *Escherichia coli*. The Gene Tailor site-directed mutagenesis kit from Invitrogen (Life Technologies) was used to mutate the TPGR site to a phospho-null (APGR) or phosphomimetic (EPGR) site. The peptides were purified on a glutathione-Sepharose 4B column and eluted using glutathione. These peptides were used in kinase assays with 4 units of human CDK1-cyclin B (New England Biolabs) or anti-CDKA IPs as the active kinase. Histone H1 (1 μg; Roche) was the positive control.

Enzyme Assays

Wild-type and mutant recombinant wheat (*Triticum aestivum*) eIF4A1 proteins were cloned in pET23d, expressed in *E. coli* BL21(DE3)pLysS, and purified on nickel-nitrilotriacetic acid agarose superflow (Qiagen) affinity columns (Mayberry et al., 2007). ATP hydrolysis by recombinant wheat eIF4A was measured by following the oxidation of NADH using a pyruvate kinase/lactate dehydrogenase coupled-enzyme assay and detecting variation of A_{340} on a Spectramax Plus microplate reader (Molecular Devices). Each 100-μL ATPase reaction contained 50 mM HEPES/KOH (pH 7.6), 2 mM dithiothreitol, 50 mM KOAc, 2 mM $Mg(OAc)_2$, 100 μg mL^{-1} acetyl-bovine serum albumin, 5% glycerol, 0.4 mM NADH, 0.8 mM phospho*enol*pyruvate, 1% (v/v) pyruvate kinase/lactate dehydrogenase mix (Sigma), 0.3 to 3 μM wild-type or mutant wheat eIF4A, with or without 5 μM poly(A) 18-mer RNA (Invitrogen). Reactions were initiated by the addition of 1 mM ATP and measured at 25°C after 1 h.

Mutants of recombinant wheat eIF4A (rWheIF4A) were produced from the wild-type eIF4A plasmid construct using the Gene Tailor site-directed mutagenesis kit from Invitrogen (Life Technologies), and their protein-folding integrity was confirmed by circular dichroism spectroscopy (Protein Characterization Facility, University of Glasgow). Antibody raised against recombinant wheat eIF4A protein was custom made by Sigma.

RNA helicase assays were performed according to Lin et al. (2008) using 44 (GGGAGAAAAACAAAACAAAACAAAACUAGCACCGUAAAGCACGC) and 10 (GCUUUACGGU) oligonucleotides mixed in the ratio 1.25:1. RNA duplexes were annealed by cooling from 95°C to 8°C at a rate of −0.5°C for 30 s over 176 cycles using an MJ PCR thermocycler.

An eIF4A-dependent wheat germ in vitro protein translation system was produced according to a method described previously for the depletion of eIF2 (Benkowski et al., 1995). A 5-mL immunoaffinity column with anti-eIF4A IgG cross-linked to a protein A matrix was prepared using the IgG Plus Orientation Kit from Pierce (Thermo Scientific) and the manufacturer's instructions. Wheat germ S30 (WGS30) was prepared as described previously (Browning and Mayberry, 2006), 7 mL was applied to the immunoaffinity column equilibrated with elution buffer [10% glycerol, 20 mM HEPES/KOH, pH 7.6, 5 mM $Mg(OAc)_2$, 120 mM KOAc, and 7 mM β-mercaptoethanol], and fractions were collected. Typically, only a maximum of 4 mL of WGS30 could be depleted of eIF4A, as judged by western blot of the fractions from the column (data not shown). The removal of eIF4A in WGS30 also reduced other eIF4A-associated factors, particularly eIF4F, which is of low abundance in wheat germ (Browning et al., 1990). In order for depleted WGS30 to recover a translation rate as close as possible to the nondepleted form, purified recombinant wheat eIF4B and eIF4F were added into the reaction (Mayberry et al., 2007). Capped mRNAs (BAA, AtHSP21, AtCyclin D3) were prepared by in vitro transcription of the linearized plasmids, and in vitro translation assays were as described previously (Benkowski et al., 1995; Browning and Mayberry, 2006). A standard reaction contains, in a volume of 50 μL, 24 mM HEPES/KOH, pH 7.6, 2.4 mM dithiothreitol, 0.1 mM spermine, 2 mM $Mg(OAc)_2$, 35 mM KCl, 95 mM KOAc, 1 mM ATP, 0.2 mM GTP, 34 μM [^{14}C]Leu, 50 μM 19 amino acids (−Leu), 7.8 mM creatine phosphate, 1.5 μg of creatine kinase, 1 μg of wheat eIF4B, 2 μg of wheat eIF4F, and 18 μL of eIF4A-depleted WGS30. The reaction was initiated by the addition of 2.5 pmol of mRNA, incubated for 30 min at 27°C, and stopped with 5% TCA. The amount of [^{14}C]Leu incorporated into polypeptide was determined as described previously (Browning and Mayberry, 2006). Assays were carried out in triplicate and averaged.

Site-Directed Mutagenesis

The full-length Arabidopsis eIF4A-1 genomic DNA fragment in pDONR207 was used to mutate Thr-164 to either Ala (T164A) or Glu (T164E). Mutations were introduced using the GENEART Site-Directed Mutagenesis System (Life Technologies) following the manufacturer's instructions and the primers listed in Supplemental Table S1. The wild-type, T164A, and T164E full-length genomic constructs were transferred into pBGWFS7 using primers AteIF4Ag attB1 and attB2 (Supplemental Table S1).

Production and Analysis of Transgenic Arabidopsis Mutant Plants

Arabidopsis *eif4a1/eIF4A1* heterozygous T-DNA insertion mutant plants (Bush et al., 2015) were transformed with *Agrobacterium tumefaciens* cells (strain GV3101) by the floral dip method (Clough and Bent, 1998). Seeds were selected in sulfadiazine and DL-phosphinothricin, and surviving seedlings homozygous for the *eIF4A1* T-DNA insertion were identified using primers GK eIF4A-1 F, GK LB T-DNA, and AteIF4A-1 3′R, and the presence of the transgene was detected with BASTA-specific primers (Supplemental Table S1).

Plants homozygous for the T-DNA insertion and containing the complementing construct were selected, and their growth phenotypes were compared with Col-0. Plants were grown in a greenhouse under long days (16 h of light/8 h of dark) or in growth rooms under short days (8 h of light/16 h of dark) as described in the figure legends. Rosette growth analysis utilized the PSI PlantScreen high-throughput phenotyping platform (Photon Systems Instruments). Eight plants per genotype were grown on two randomized trays (5 × 4 grid). Image data were acquired every day using the PlantScreen VIS top view camera (UI-1480RE-C; sensor size, 2,560 × 1,920 pixels; lens, 8-mm f1:1) at a working distance of 580 mm. Plant rosette (top view) morphometric and RGB analyses were conducted using the on-system PSI software. Average rosette area ± SE was calculated across genotype and over the time period.

Seedlings for root and cellular measurements were grown at 25°C in a growth cabinet and assessed as described by Bush et al. (2015).

Quantitative PCR

To determine the abundance of the eIF4A transcript in the transgenic lines, RNA was extracted from 8-d-old seedlings grown in petri dishes. For quantitative PCR, 23-d-old rosettes were used for RNA extraction. For the analysis of flowering genes, RNA was extracted from 10-d-old seedlings grown in petri dishes in short days (16 h of dark/8 h of light) or long days (16 h of light/8 h of dark). RNA was extracted using the RNeasy Plant Mini kit (Qiagen), and 1 μg of RNA was used for the RT reaction using SuperScriptIII reverse transcriptase (Invitrogen). The primers used for PCR are listed in Supplemental Table S1. Quantitative PCR was performed using the LightCycler 480 II (Roche) with 10 ng of complementary DNA template and LightCycler 480 SYBR Green Master following the manufacturer's protocol, and relative quantification was done using the LightCycler 480 II software using ACTIN2 as a reference gene.

Yeast Two-Hybrid Assays

Gateway-compatible complementary DNA clones corresponding to eIF4A and other cap-binding proteins, CDKA (Bush et al., 2009), CDKB2.1, CDKC1, and CDKD1, were transferred from pDONR207 into yeast two-hybrid vectors, and interactions were assessed as described previously (Rossignol et al., 2007).

Arabidopsis and BY2 Cell Culture Synchronization

Arabidopsis cells were maintained as described previously (Hutchins et al., 2004) and synchronized by Suc starvation according to Menges and Murray (2002), whereas tobacco (*Nicotiana tabacum*) BY2 cells were semisynchronized by simple dilution of 10-d-old culture into fresh BY2 medium at a 1:10 ratio (Koroleva et al., 2004). Flow cytometric analyses and mitotic index estimates were performed according to Koroleva et al. (2004). BY2 synchronization was performed according to Kumagai-Sano et al. (2006).

Accession Numbers

The accession numbers for the genes used for this article are as follows: *At3g13920* (*AteIF4A1*), *At1g54270* (*AteIF4A2*), *At3g48750* (*AtCDKA*), *At1g76540* (*AtCDKB2.1*), *At5g10270* (*AtCDKC1*), *At1g73690* (*AtCDKD1*), *At3g26400* (*AteIF4B2*), *At4g18040* (*AteIF4E*), *At5g35620* (*AteIFiso4E*), *At3g60240* (*AteIF4G*), *At5g57870* (*AteIFiso4G1*), *At2g24050* (*AteIFiso4G2*), *At4g27670* (*AtHSP21*), and *At4g34160* (*AtCyclin D3.1*).

Supplemental Data

The following supplemental materials are available.

Supplemental Figure S1. CDK interactions with eIF4A1 and eIF4A2 in yeast two-hybrid assays.

Supplemental Figure S2. ClustalW (1.81) multiple sequence alignments showing that the TPGR CDKA phosphorylation site is conserved across eukaryotes.

Supplemental Figure S3. Effect of the *eif4a1* mutation on root growth.

Supplemental Figure S4. Loss of eIF4A affects flowering time and flowering time gene expression.

Supplemental Figure S5. Quantitative PCR and RT-PCR expression analysis of eIF4A phosphosite variants.

Supplemental Table S1. Primer sequence information.

ACKNOWLEDGMENTS

We thank Dr. Sharon M. Kelly (University of Glasgow) for circular dichroism spectroscopic analysis of recombinant wheat eIF4A1 proteins, William Merrick for suggestions to optimize the RNA helicase assays, Henrik Buschmann for insightful discussions, the NPPC staff for automated data acquisition, and the horticultural staff for plant husbandry.

Received March 31, 2016; accepted July 5, 2016; published July 7, 2016.

LITERATURE CITED

Andreou AZ, Klostermeier D (2013) The DEAD-box helicase eIF4A: paradigm or the odd one out? RNA Biol **10:** 19–32

Benkowski LA, Ravel JM, Browning KS (1995) Development of an in vitro translation system from wheat germ that is dependent upon the addition of eukaryotic initiation factor 2. Anal Biochem **232:** 140–143

Benz J, Trachsel H, Baumann U (1999) Crystal structure of the ATPase domain of translation initiation factor 4A from Saccharomyces cerevisiae: the prototype of the DEAD box protein family. Structure **7:** 671–679

Bi X, Goss DJ (2000) Wheat germ poly(A)-binding protein increases the ATPase and the RNA helicase activity of translation initiation factors eIF4A, eIF4B, and eIF-iso4F. J Biol Chem **275:** 17740–17746

Boex-Fontvieille E, Daventure M, Jossier M, Zivy M, Hodges M, Tcherkez G (2013) Photosynthetic control of Arabidopsis leaf cytoplasmic translation initiation by protein phosphorylation. PLoS ONE **8:** e70692

Bordeleau ME, Cencic R, Lindqvist L, Oberer M, Northcote P, Wagner G, Pelletier J (2006a) RNA-mediated sequestration of the RNA helicase eIF4A by pateamine A inhibits translation initiation. Chem Biol **13:** 1287–1295

Bordeleau ME, Mori A, Oberer M, Lindqvist L, Chard LS, Higa T, Belsham GJ, Wagner G, Tanaka J, Pelletier J (2006b) Functional characterization of IRESes by an inhibitor of the RNA helicase eIF4A. Nat Chem Biol **2:** 213–220

Boudet N, Aubourg S, Toffano-Nioche C, Kreis M, Lecharny A (2001) Evolution of intron/exon structure of DEAD helicase family genes in Arabidopsis, Caenorhabditis, and Drosophila. Genome Res **11:** 2101–2114

Browning KS, Bailey-Serres J (2015) Mechanism of cytoplasmic mRNA translation. The Arabidopsis Book **13:** e0176, doi/10.1199/tab.0176

Browning KS, Humphreys J, Hobbs W, Smith GB, Ravel JM (1990) Determination of the amounts of the protein synthesis initiation and elongation factors in wheat germ. J Biol Chem **265:** 17967–17973

Browning KS, Mayberry L (2006) In vitro translation of plant viral RNA. Curr Protoc Microbiol **Chapter 16:** Unit 16K 11

Bush MS, Crowe N, Zheng T, Doonan JH (2015) The RNA helicase, eIF4A-1, is required for ovule development and cell size homeostasis in Arabidopsis. Plant J **84:** 989–1004

Bush MS, Hutchins AP, Jones AM, Naldrett MJ, Jarmolowski A, Lloyd CW, Doonan JH (2009) Selective recruitment of proteins to 5′ cap complexes during the growth cycle in Arabidopsis. Plant J **59:** 400–412

Carberry SE, Darzynkiewicz E, Goss DJ (1991) A comparison of the binding of methylated cap analogues to wheat germ protein synthesis initiation factors 4F and (iso)4F. Biochemistry **30:** 1624–1627

Clough SJ, Bent AF (1998) Floral dip: a simplified method for Agrobacterium-mediated transformation of Arabidopsis thaliana. Plant J **16:** 735–743

Dennis MD, Browning KS (2009) Differential phosphorylation of plant translation initiation factors by Arabidopsis thaliana CK2 holoenzymes. J Biol Chem **284:** 20602–20614

Dissmeyer N, Weimer AK, Pusch S, De Schutter K, Alvim Kamei CL, Nowack MK, Novak B, Duan GL, Zhu YG, De Veylder L, et al (2009) Control of cell proliferation, organ growth, and DNA damage response operate independently of dephosphorylation of the *Arabidopsis* Cdk1 homolog CDKA;1. Plant Cell **21:** 3641–3654

Dobrikov MI, Shveygert M, Brown MC, Gromeier M (2014) Mitotic phosphorylation of eukaryotic initiation factor 4G1 (eIF4G1) at Ser1232 by Cdk1:cyclin B inhibits eIF4A helicase complex binding with RNA. Mol Cell Biol **34:** 439–451

Durand E, Bouchet S, Bertin P, Ressayre A, Jamin P, Charcosset A, Dillmann C, Tenaillon MI (2012) Flowering time in maize: linkage and epistasis at a major effect locus. Genetics **190:** 1547–1562

Durek P, Schmidt R, Heazlewood JL, Jones A, MacLean D, Nagel A, Kersten B, Schulze WX (2010) PhosPhAt: the Arabidopsis thaliana phosphorylation site database. An update. Nucleic Acids Res **38:** D828–D834

Eliscovich C, Peset I, Vernos I, Méndez R (2008) Spindle-localized CPE-mediated translation controls meiotic chromosome segregation. Nat Cell Biol **10:** 858–865

Fehler O, Singh P, Haas A, Ulrich D, Müller JP, Ohnheiser J, Klempnauer KH (2014) An evolutionarily conserved interaction of tumor suppressor protein Pdcd4 with the poly(A)-binding protein contributes to translation suppression by Pdcd4. Nucleic Acids Res **42:** 11107–11118

Gaamouche T, Manes CL, Kwiatkowska D, Berckmans B, Koumproglou R, Maes S, Beeckman T, Vernoux T, Doonan JH, Traas J, et al (2010) Cyclin-dependent kinase activity maintains the shoot apical meristem cells in an undifferentiated state. Plant J **64:** 26–37

Gallie DR, Browning KS (2001) eIF4G functionally differs from eIFiso4G in promoting internal initiation, cap-independent translation, and translation of structured mRNAs. J Biol Chem **276:** 36951–36960

Heazlewood JL, Durek P, Hummel J, Selbig J, Weckwerth W, Walther D, Schulze WX (2008) PhosPhAt: a database of phosphorylation sites in Arabidopsis thaliana and a plant-specific phosphorylation site predictor. Nucleic Acids Res **36:** D1015–D1021

Hemerly A, Engler JdeA, Bergounioux C, Van Montagu M, Engler G, Inzé D, Ferreira P (1995) Dominant negative mutants of the Cdc2 kinase uncouple cell division from iterative plant development. EMBO J **14:** 3925–3936

Hinnebusch AG (2014) The scanning mechanism of eukaryotic translation initiation. Annu Rev Biochem **83:** 779–812

Hutchins AP, Roberts GR, Lloyd CW, Doonan JH (2004) In vivo interaction between CDKA and eIF4A: a possible mechanism linking translation and cell proliferation. FEBS Lett **556:** 91–94

Jackson RJ, Hellen CU, Pestova TV (2010) The mechanism of eukaryotic translation initiation and principles of its regulation. Nat Rev Mol Cell Biol **11:** 113–127

Jung H, Gkogkas CG, Sonenberg N, Holt CE (2014) Remote control of gene function by local translation. Cell **157:** 26–40

Kõivomägi M, Valk E, Venta R, Iofik A, Lepiku M, Morgan DO, Loog M (2011) Dynamics of Cdk1 substrate specificity during the cell cycle. Mol Cell **42:** 610–623

Koroleva OA, Calder G, Pendle AF, Kim SH, Lewandowska D, Simpson CG, Jones IM, Brown JW, Shaw PJ (2009) Dynamic behavior of *Arabidopsis* eIF4A-III, putative core protein of exon junction complex: fast relocation to nucleolus and splicing speckles under hypoxia. Plant Cell **21:** 1592–1606

Koroleva OA, Tomlinson M, Parinyapong P, Sakvarelidze L, Leader D, Shaw P, Doonan JH (2004) CycD1, a putative G1 cyclin from *Antirrhinum majus*, accelerates the cell cycle in cultured tobacco BY-2 cells by enhancing both G1/S entry and progression through S and G2 phases. Plant Cell **16:** 2364–2379

Kumagai-Sano F, Hayashi T, Sano T, Hasezawa S (2006) Cell cycle synchronization of tobacco BY-2 cells. Nat Protoc **1:** 2621–2627

Le H, Browning KS, Gallie DR (1998) The phosphorylation state of the wheat translation initiation factors eIF4B, eIF4A, and eIF2 is differentially regulated during seed development and germination. J Biol Chem **273:** 20084–20089

Lin D, Pestova TV, Hellen CU, Tiedge H (2008) Translational control by a small RNA: dendritic BC1 RNA targets the eukaryotic initiation factor 4A helicase mechanism. Mol Cell Biol **28:** 3008–3019

Linder P, Fuller-Pace FV (2013) Looking back on the birth of DEAD-box RNA helicases. Biochim Biophys Acta **1829:** 750–755

Lu WT, Wilczynska A, Smith E, Bushell M (2014) The diverse roles of the eIF4A family: you are the company you keep. Biochem Soc Trans **42:** 166–172

Marintchev A (2013) Roles of helicases in translation initiation: a mechanistic view. Biochim Biophys Acta **1829:** 799–809

Mayberry LK, Allen ML, Dennis MD, Browning KS (2009) Evidence for variation in the optimal translation initiation complex: plant eIF4B, eIF4F, and eIF(iso)4F differentially promote translation of mRNAs. Plant Physiol **150:** 1844–1854

Mayberry LK, Allen ML, Nitka KR, Campbell L, Murphy PA, Browning KS (2011) Plant cap-binding complexes eukaryotic initiation factors eIF4F and eIFISO4F: molecular specificity of subunit binding. J Biol Chem **286:** 42566–42574

Mayberry LK, Dennis MD, Allen ML, Nitka KR, Murphy PA, Campbell L, Browning KS (2007) Expression and purification of recombinant wheat translation initiation factors eIF1, eIF1A, eIF4A, eIF4B, eIF4F, eIF (iso)4F, and eIF5. Methods Enzymol **430:** 397–408

Mead EJ, Masterton RJ, von der Haar T, Tuite MF, Smales CM (2014) Control and regulation of mRNA translation. Biochem Soc Trans **42:** 151–154

Menges M, Murray JA (2002) Synchronous Arabidopsis suspension cultures for analysis of cell-cycle gene activity. Plant J **30:** 203–212

Merrick WC (2015) eIF4F: a retrospective. J Biol Chem **290:** 24091–24099

Montanaro L, Pandolfi PP (2004) Initiation of mRNA translation in oncogenesis: the role of eIF4E. Cell Cycle **3:** 1387–1389

Obaya AJ, Sedivy JM (2002) Regulation of cyclin-Cdk activity in mammalian cells. Cell Mol Life Sci **59:** 126–142

Parsyan A, Svitkin Y, Shahbazian D, Gkogkas C, Lasko P, Merrick WC, Sonenberg N (2011) mRNA helicases: the tacticians of translational control. Nat Rev Mol Cell Biol **12:** 235–245

Pause A, Sonenberg N (1992) Mutational analysis of a DEAD box RNA helicase: the mammalian translation initiation factor eIF-4A. EMBO J **11:** 2643–2654

Pierrat OA, Mikitova V, Bush MS, Browning KS, Doonan JH (2007) Control of protein translation by phosphorylation of the mRNA 5′-cap-binding complex. Biochem Soc Trans **35:** 1634–1637

Pyronnet S, Dostie J, Sonenberg N (2001) Suppression of cap-dependent translation in mitosis. Genes Dev **15:** 2083–2093

Quesada V, Macknight R, Dean C, Simpson GG (2003) Autoregulation of FCA pre-mRNA processing controls Arabidopsis flowering time. EMBO J **22:** 3142–3152

Rogers GW Jr, Komar AA, Merrick WC (2002) eIF4A: the godfather of the DEAD box helicases. Prog Nucleic Acid Res Mol Biol **72:** 307–331

Rossignol P, Collier S, Bush M, Shaw P, Doonan JH (2007) Arabidopsis POT1A interacts with TERT-V(I8), an N-terminal splicing variant of telomerase. J Cell Sci **120:** 3678–3687

Roy B, von Arnim AG (2013) Translational regulation of cytoplasmic mRNAs. The Arabidopsis Book **11:** e0165, doi/10.1199/tab.0165

Ruud KA, Kuhlow C, Goss DJ, Browning KS (1998) Identification and characterization of a novel cap-binding protein from Arabidopsis thaliana. J Biol Chem **273:** 10325–10330

Sonenberg N, Gingras AC (1998) The mRNA 5′ cap-binding protein eIF4E and control of cell growth. Curr Opin Cell Biol **10:** 268–275

Stoneley M, Willis AE (2015) eIF4A1 is a promising new therapeutic target in ER-negative breast cancer. Cell Death Differ **22:** 524–525

Takeda DY, Wohlschlegel JA, Dutta A (2001) A bipartite substrate recognition motif for cyclin-dependent kinases. J Biol Chem **276:** 1993–1997

Tuteja N, Vashisht AA, Tuteja R (2008) Translation initiation factor 4A: a prototype member of dead-box protein family. Physiol Mol Biol Plants **14:** 101–107

Ubersax JA, Ferrell JE Jr (2007) Mechanisms of specificity in protein phosphorylation. Nat Rev Mol Cell Biol **8:** 530–541

Umezawa T, Sugiyama N, Takahashi F, Anderson JC, Ishihama Y, Peck SC, Shinozaki K (2013) Genetics and phosphoproteomics reveal a protein phosphorylation network in the abscisic acid signaling pathway in Arabidopsis thaliana. Sci Signal **6:** rs8

Vain P, Thole V, Worland B, Opanowicz M, Bush MS, Doonan JH (2011) A T-DNA mutation in the RNA helicase eIF4A confers a dose-dependent dwarfing phenotype in Brachypodium distachyon. Plant J **66:** 929–940

Valásek LS (2012) 'Ribozoomin': translation initiation from the perspective of the ribosome-bound eukaryotic initiation factors (eIFs). Curr Protein Pept Sci **13:** 305–330

Wang X, Bian Y, Cheng K, Gu LF, Ye M, Zou H, Sun SS, He JX (2013) A large-scale protein phosphorylation analysis reveals novel phosphorylation motifs and phosphoregulatory networks in Arabidopsis. J Proteomics **78:** 486–498

Webster C, Gaut RL, Browning KS, Ravel JM, Roberts JKM (1991) Hypoxia enhances phosphorylation of eukaryotic initiation factor 4A in maize root tips. J Biol Chem **266:** 23341–23346

Wu XN, Sanchez Rodriguez C, Pertl-Obermeyer H, Obermeyer G, Schulze WX (2013) Sucrose-induced receptor kinase SIRK1 regulates a plasma membrane aquaporin in Arabidopsis. Mol Cell Proteomics **12:** 2856–2873

Zacharaki V, Benhamed M, Poulios S, Latrasse D, Papoutsoglou P, Delarue M, Vlachonasios KE (2012) The Arabidopsis ortholog of the YEATS domain containing protein YAF9a regulates flowering by controlling H4 acetylation levels at the FLC locus. Plant Sci **196:** 44–52

Zhang H, Zhou H, Berke L, Heck AJ, Mohammed S, Scheres B, Menke FL (2013) Quantitative phosphoproteomics after auxin-stimulated lateral root induction identifies an SNX1 protein phosphorylation site required for growth. Mol Cell Proteomics **12:** 1158–1169

Zulawski M, Braginets R, Schulze WX (2013) PhosPhAt goes kinases: searchable protein kinase target information in the plant phosphorylation site database PhosPhAt. Nucleic Acids Res **41:** D1176–D1184